

Fast and Accurate Quantification of T1, T2 and Proton Density using IR bSSFP with Slice Profile Correction and Model Based Reconstruction

Andreas Lesch¹, Andreas Petrovic¹, Tilman Johannes Sumpf², Christoph Stefan Aigner¹, and Rudolf Stollberger¹

¹Department for Medical Engineering, Graz University of Technology, Graz, Styria, Austria, ²Biomedizinische NMR Forschungs GmbH, Max-Planck-Institut für biophysikalische Chemie, Göttingen, Germany

Target Audience: Engineers and scientists interested in quantitative MRI

Introduction: Fast and accurate quantification of NMR parameters is an essential basis for biomarker imaging. A fast method for multiple parameter quantification was presented by Schmitt [1], which uses the transient response of the inversion recovery (IR) bSSFP sequence to quantify T₁, T₂ and spin density with one measurement. A drawback of this method is that the quantification accuracy decreases substantially (especially in T₂) if the slice profile deviates from the desired rectangular shape. The RF-pulses used in the bSSFP sequence usually provide a rather non-ideal slice profile, because it is tried to keep TR as low as possible. The aim of this work was both to correct these slice profile effects to increase the quantification accuracy and to further accelerate this method by a combination of under-sampling and model-based image reconstruction. Model-based image reconstruction integrates parameter estimation in the reconstruction process.

Theory and Methods: The reconstruction of the under-sampled segmented encodings is performed in k-space using a model-based nonlinear inverse reconstruction scheme presented by Sumpf [2]. This approach is based on a cost function (Eq. 1) that reconstructs the complete parameter set \mathbf{T} at once (Eq. 2). \mathbf{S}_n is the underlying unknown image at time point n , the matrix \mathbf{P} describes the applied under-sampling pattern, \mathbf{C}_c is the coil sensitivity of receiver coil c , N_{ph} and N_c are the number of acquired images sampling the transient time course and the number of receiver coils, respectively. N_{seg} is the number of k-space lines acquired per inversion in each of the N_{ph} images. The forward model is calculated using the Bloch Equations (Eq. 4) assuming no relaxation during excitation, where \mathbf{E} and \vec{e} describe the transverse and longitudinal relaxation between two excitations (Eq. 5 and 6), \mathbf{R}_x describes the excitation as a rotation around the x-axis and the rotation around z by π considers the alternating excitation of the sequence. To consider slice profile effects, the measured slice profile was discretized into K sub slices. \vec{M}_j is the resulting magnetization vector at the readout after the j^{th} excitation as the vector sum over all sub slices. For minimization of Eq. 1 the CG-Descend method described in [3] was used. The solver is initialized with parameter maps calculated using the equations of Schmitt [1]. The cost function's gradient was calculated by the gradient scheme described in [2] and the gradient of \vec{M}_j was obtained using the implicit function theorem [4]. As initial condition for the time course of the magnetization a full inversion of M_0 is assumed (Eq. 7), which can be justified due to adiabatic inversion and gradient spoiling after the inversion.

$$\vec{T} = \text{argmin} \frac{1}{2} \sum_{c=1}^{N_c} \sum_{n=1}^{N_{ph}} \left\| \mathbf{P} \cdot \text{DFT} \{ \mathbf{S}_n(n, \vec{T}) \cdot \mathbf{C}_c \} - \mathbf{S}_{data}(n, c) \right\|_2^2 \quad (1)$$

$$\vec{T} = (\vec{T}_1(\vec{x}), \vec{T}_2(\vec{x}), \vec{M}_0(\vec{x})) \quad (2)$$

$$\vec{M}_j = \frac{1}{K} \sum_{k=1}^K \vec{M}_{j,k} = \frac{1}{K} \sum_{k=1}^K \mathbf{E} \mathbf{R}_x(\alpha_{j,k}) \mathbf{R}_z(\pi) (\mathbf{E} \vec{M}_{j-1} + \vec{e}) + \vec{e} \quad (4)$$

$$\mathbf{E} = \text{diag} \left(e^{-\frac{TE}{T_2}}, e^{-\frac{TE}{T_2}}, e^{-\frac{TE}{T_1}} \right) \quad (5)$$

$$\mathbf{S}_u(n, \vec{x}) = \vec{M}_{t,f} \text{ if } j \bmod N_{seg} = 0 \text{ and } n = \frac{j}{N_{seg}} \quad (3)$$

$$\vec{e} = \left(0, 0, 1 - e^{-\frac{TE}{T_1}} \right) \cdot M_0 \quad (6)$$

$$\vec{M}_0 = (0, 0, -M_0) \quad (7)$$

The study was performed on a clinical 3T system (Magnetom Skyra, Siemens, Erlangen, Germany). Measurements were performed on an agar phantom with a FOV of 70mm, 5mm slice thickness and a single channel receiver coil. In-vivo cerebral measurements were performed on healthy volunteers using a 20-channel Head/Neck coil (Siemens, Erlangen, Germany), a FOV of 200mm, a matrix size of 128x128 and a slice thickness of 5mm. The acquisition starts after a delay of 105ms (inversion and preparation) with a TR of 4.3ms and $N_{seg}=8$ k-space lines were acquired per image. A delay of 8.1s ensures complete relaxation before the next inversion. For the reconstruction the slice profile was discretized into 36 sub slices. The quantitative results were compared to reference measurements using standard procedures (T₁: IR-TSE; T₂ in-vivo: multiple SE sequence (MSE), phantom T₂: SE-sequence with different TEs). The reference measurements were evaluated using a three parameter and a two parameter mono-exponential fit for T₁ and T₂ respectively. The uncorrected parameter map was generated using the analytical expressions proposed by Schmitt [1]. The parameter quantification was done using MATLAB (Mathworks Inc., Natick, USA, v7.12.0). The under-sampled data were generated retrospectively using a blocked under-sampling pattern. The influence in plane of B₁-field inhomogeneity was corrected using the Double Angle Method described in [5].

Results: Fig. 1 shows the achieved parameter maps of the phantom measurement with a single channel receiver coil and different acceleration factors compared to the reference measurement and the uncorrected results. In comparison to the reference measure the error in T₁ is in the same range below 10% for the corrected and uncorrected case (Tab. 1). For T₂, the error without slice profile correction is very high (>90%), but it can be reduced with the described method into the range below 10%. For single channel coil measurements, the under-sampling has nearly no effect on the quantification accuracy up to an acceleration factor of 3. Aliasing artifacts start to appear at an acceleration factor of 4, but the error is still low and increases slightly with increasing acceleration. Fig. 2 shows the in-vivo measurements with parallel imaging (20 channel coil) for T₁ and T₂ using an acceleration factor of 9.

Discussion and Conclusion: The phantom measurements show that influence of the non-ideal slice profile can be corrected. With model based reconstruction and a single receiver coil acceleration factors up to 4 can be used. At higher acceleration factors increasing artifacts corrupt the quantification. For the used multichannel receiver coil an acceleration factors of 9 delivers reasonable image quality (Fig. 2). The influence of the under-sampling pattern is also important as described in [2]. A standard interleaved pattern results in stronger artifacts and restricts the acceleration factor to 5. The discretization of the slice profile with K=36 sub slices is sufficient as dedicated investigations have shown. For in-vivo measurements an on-resonant magnetization transfer (MT) effect was observed. MT reduces the steady state signal [6] and changes the shape of the transient decay. This effect is responsible for an overestimation of T₁ by about 10-15% and an underestimation of T₂ by about 65-75% in brain tissue. For in-vivo application, these MT effects must be considered as well which is part of ongoing work. Furthermore, it is tried to extend the presented method to quantify also MT. The chosen shot interval with 8.1s is sufficiently long for all tissues in the examined part of the body except CSF.

References: [1] Schmitt et al. MRM 51:661-667 (2004), [2] Sumpf et al. JMRI 34(2):420-428 (2011), [3] Hager, Zhang SIAM J Optim 16(1):170-192 (2005) [4] Hager et al. Journal on Optimization 16:170-192 (2005), [5] Stollberger et al. MRM 35(2):246-251 (1996), [6] Bieri et al. MRM 56:1067-1074 (2006)

Acknowledgement: This work was funded by the Austrian Science Fund "SFB 3209-18"

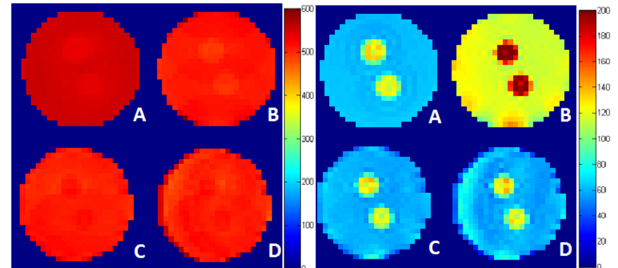


Fig. 1: T₁ maps (left) and T₂ maps (right): (A) reference measurement; (B) uncorrected method of Schmitt; (C) slice profile corrected with acc = 3; (D) slice profile corrected with acc = 6

	T ₁ in ms		T ₂ in ms		M ₀ in a.u.
Reference	552±2.9		62.2±1.8		0.89±0.03
Schmitt	514±7.2	-6.9%	118.8±5.7	+91.0%	0.80±0.12
acc = 1	514±6.3	-6.9%	61.0±2.3	-1.9%	0.80±0.05
acc = 2	513±6.3	-7.0%	61.7±2.3	-0.7%	0.79±0.05
acc = 4	509±8.9	-7.8%	64.6±5.3	+3.9%	0.70±0.06
acc = 6	500±10.1	-9.4%	70.5±6.5	+13.4%	0.66±0.06

Tab. 1: Mean, standard deviation and the difference to the reference measurement of the quantified parameter maps with different acceleration factors inside a ROI of the phantom.

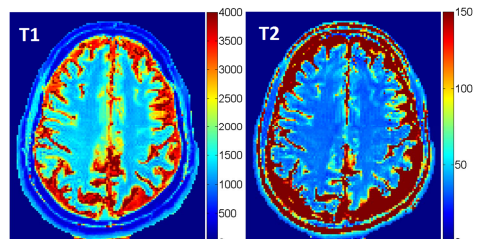


Fig. 2: Acquired parameter maps (T₁ and T₂) in-vivo applying 9 times under-sampling.